the mixture, and the solvent was reduced to ca. 2 cm^3 by using a vacuum line.

The mixture was placed at −10 °C for 14 h and yielded some mauve/black crystals. These were isolated by filtration, quickly washed with $CFCl_3$ (4 × 5 cm^3) at 0 °C, and dried in vacuo.

All measurements were made on freshly prepared samples. When necessary, samples were stored in sealed tubes at −20 °C in the dark.

EXAFS. EXAFS data at the iron K-edge were recorded at the Daresbury Synchrotron Radiation Source operating at an energy of 2.0 GeV with an average current of 160 mA. Transmission EXAFS data were recorded upon freshly prepared (~24 h old) samples at room temperature, which had been stored at ca. −10 °C in the dark, the samples being placed between "Sellotape" strips. Powdered samples ca. 0.5 mm thick were used, and two or three data sets were recorded upon each sample. No changes in the EXAFS were evident with successive scans, indicating no significant decomposition during the data collection.

Acknowledgment. We thank the SERC for support, for research studentships (to S.J.H. and S.K.H.), and for an allocation of the EXAFS service. The Director of the Daresbury Laboratory is thanked for the provision of facilities. We also thank Professor C. D. Garner, Dr. S. S. Hasnain, and Dr. J. Evans for discussions and Dr. D. Pletcher for assistance with the electrochemical studies.

Registry No. $[Fe(o\text{-}C_6H_4(PMe_2)_2)_2Cl_2][BF_4]_2$, 99686-48-3; $[Fe(o\text{-}C_6H_4(PMe_2)_2)_2Br_2][BF_4]_2$, 101566-59-0; $[Fe(o\text{-}C_6H_4(PMe_2)(AsMe_2))_2Cl_2][BF_4]_2$, 101566-61-4; $[Fe(o\text{-}C_6H_4(PMe_2)(AsMe_2))_2Br_2][BF_4]_2$, 101566-63-6; $[Fe(o\text{-}C_6H_4(AsMe_2)_2)_2Cl_2][BF_4]_2$, 29560-86-9; $[Fe(o\text{-}C_6H_4(AsMe_2)_2)_2Br_2][BF_4]_2$, 54512-27-5; $[Fe(Me_2PCH_2CH_2PMe_2)_2Cl_2][BF_4]_2$, 101566-65-8; $[Fe(o\text{-}C_6H_4(PMe_2)_2)_2Cl_2]$, 60536-64-3; $[Fe(o\text{-}C_6H_4(PMe_2)_2)_2Cl_2][BF_4]$, 99686-47-2; $[Fe(o\text{-}C_6H_4(PMe_2)_2)_2Br_2][BF_4]$, 60489-54-5; $[Fe(o\text{-}C_6H_4(PMe_2)(AsMe_2))_2Cl_2][BF_4]$, 101566-67-0; $[Fe(o\text{-}C_6H_4(PMe_2)(AsMe_2))_2Br_2][BF_4]$, 101566-69-2; $[Fe(o\text{-}C_6H_4(AsMe_2)_2)_2Cl_2][BF_4]$, 37817-55-3; $[Fe(o\text{-}C_6H_4(AsMe_2)_2)_2Br_2][BF_4]$, 51417-92-6; $[Fe(Me_2PCH_2CH_2PMe_2)_2Cl_2][BF_4]$, 101566-70-5; $[Fe(Me_2PCH_2CH_2PMe_2)_2Br_2][BF_4]$, 101566-72-7; $[Fe(o\text{-}C_6F_4(PMe_2)_2)_2Cl_2][BF_4]$, 97134-91-3; $[Fe(o\text{-}C_6F_4(PMe_2)_2)_2Br_2][BF_4]$, 101566-74-9; $[Fe(Me_2PCH_2CH_2PMe_2)_2Br_2][BF_4]_2$, 101566-76-1; $[Fe(o\text{-}C_6F_4(PMe_2)_2)_2Cl_2][BF_4]_2$, 101692-80-2; $[Fe(o\text{-}C_6F_4(PMe_2)_2)_2Br_2][BF_4]_2$, 101566-78-3; $[Fe(o\text{-}C_6H_4(PMe_2)_2)_2Br_2]$, 60489-95-4; $[Fe(o\text{-}C_6H_4(PMe_2)(AsMe_2))_2Cl_2]$, 101566-79-4; $[Fe(o\text{-}C_6F_4(PMe_2)_2)_2Cl_2]$, 60536-64-3; $[Fe(o\text{-}C_6H_4(PPh_2)_2)_2Cl_2]$, 101566-80-7; $[Fe(Me_2PCH_2CH_2PMe_2)_2Cl_2]$, 27316-95-6; $[Fe(Me_2PCH_2CH_2PMe_2)_2Br_2]$, 101566-81-8; $[Fe(o\text{-}C_6H_4(PPh_2)_2)_2Cl_2][BF_4]$, 101566-83-0; $[Fe(o\text{-}C_6H_4(PPh_2)_2)_2Cl_2][BF_4]_2$, 101566-85-2; $[Ph_4P][FeCl_4]$, 30862-67-0; $[Fe(o\text{-}C_6H_4(PPh_2)_2)_2Br_2]$, 101566-86-3.

Contribution from the Department of Chemistry, University of Rochester, Rochester, New York 14627

Preparation and Structural Comparison of the Ruthenium(0) Derivatives $Ru(DMPE)_2L$ (L = PMe_3, CO; DMPE = 1,2-Bis(dimethylphosphino)ethane)

William D. Jones*† and Emanuela Libertini

Received September 3, 1985

The thermal reaction of $Ru(DMPE)_2(nap)H$ (DMPE = 1,2-bis(dimethylphosphino)ethane; nap = naphthyl) with PMe_3 results in the formation of the new zerovalent derivative $Ru(DMPE)_2(PMe_3)$. The molecule crystallizes in orthorhombic space group *Pnam* with $Z = 4$ (d_{calcd} = 1.38 g/cm^3) and lattice parameters a = 16.3540 (18) Å, b = 9.3240 (30) Å, and c = 16.0210 (23) Å. The structure displays a square-pyramidal geometry in which the PMe_3 occupies the apical position. Separate modeling of two disorders due to 4-fold rotation of the DMPE ligands about the apical Ru–P vector and 2-fold rotation of the PMe_3 ligand gives refinement to R_1 = 0.042, R_2 = 0.066. Some reactions of the low-valent derivative are reported. Displacement of PMe_3 by CO occurs at 25 °C, producing $Ru(DMPE)_2(CO)$. Similarly, $P(CD_3)_3$ exchanges with coordinated PMe_3 more slowly. Neopentyl isocyanide slowly displaces PMe_3 at higher temperatures to give the isocyanide derivative. The CO adduct crystallizes in orthorhombic space group *Pbca* with Z = 16 and lattice parameters a = 19.110 (9) Å, b = 23.116 (6) Å, and c = 18.780 (6) Å, the non-hydrogen atoms being refined to R_1 = 0.048, R_2 = 0.066. A trigonal-bipyramidal geometry is observed in which the CO occupies an equatorial site. The mechanism of substitution indicates both associative and dissociative pathways.

Introduction

The tremendous reactivity of transition-metal complexes in lower oxidation states has resulted in a wide variety of oxidative-addition chemistry of these low-valent metal derivatives.[1] The reducing capability of these metals is found to be affected by the ligands attached to the metal. Good donor ligands such as hydride, η^5-cyclopentadienyl, and trialkylphosphine are all found to effectively increase the electron density on the metal center, whereas electron-withdrawing ligands such as CO or PF_3 reduce the tendency of the metal to act as a reducing agent.

Both iron(0) and ruthenium(0) complexes are known to be very reactive toward the oxidative addition of C–H bonds.[2-7] Twenty years ago Chatt reported the preparation of $Ru(DMPE)_2(nap)H$ (DMPE = 1,2-bis(dimethylphosphino)ethane; nap = naphthyl) by the reduction of $Ru(DMPE)_2Cl_2$ with sodium naphthalenide. The former complex was observed to undergo reductive elimination of naphthalene at 60 °C to produce a reactive 16-electron ruthenium(0) intermediate that would react with other aromatic C–H bonds (eq 1).[2] The related iron complex $[Fe(PMe_3)_4]$ was

$$Ru(DMPE)_2(nap)H \xrightarrow[-C_{10}H_8]{} [Ru(DMPE)_2] \xrightarrow[ArH]{} Ru(dmpe)_2(Ar)H \quad (1)$$

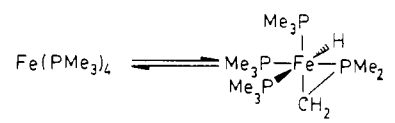

(2)

prepared by both Muetterties[4] and Karsch and Klein[5] and was found to be in equilibrium with the internally metalated species (eq 2). The analogous chemistry with the PMe_3 derivatives of

† A. P. Sloan Fellow, 1984–1986, and Camille and Henry Dreyfus Teacher-Scholar, 1985–1987.

(1) Halpern, J. *Acc. Chem. Res.* **1970**, *3*, 386–392. Collman, J. P.; Hegedus, L. S. *Principles and Applications of Organotransition Metal Chemistry*; University Science: Mill Valley, CA, 1980.
(2) Chatt, J.; Davidson, J. M. *J. Chem. Soc.* **1965**, 843–855.
(3) Ittel, S. D.; Tolman, C. A.; English, A. D.; Jesson, J. P. *J. Am. Chem. Soc.* **1976**, *98*, 6073–6075. Tolman, C. D.; Ittel, S. D.; English, A. D.; Jesson, J. P. *J. Am. Chem. Soc.* **1979**, *101*, 1742–1751. Ittel, S. D.; Tolman, C. A.; English, A. D.; Jesson, J. P. *J. Am. Chem. Soc.* **1978**, *100*, 7577–7585.
(4) Rathke, J. W.; Muetterties, E. L. *J. Am. Chem. Soc.* **1975**, *97*, 3272–3273.
(5) Karsch, H. H.; Klein, H. F.; Schmidbaur, H. *Chem. Ber.* **1977**, *110*, 2200–2210.
(6) Morris, R. H.; Shiralian, M. *J. Organomet. Chem.* **1984**, *260*, C47–C51.
(7) Werner, H.; Werner, R. *J. Organomet. Chem.* **1981**, *209*, C60–C64. Werner, H.; Gotzig, J. *Organometallics* **1983**, *2*, 547–549.

0020-1669/86/1325-1794$01.50/0

ruthenium and osmium was later reported by Werner.[7]

The study presented here describes the trapping of the reactive intermediate in Chatt's system with the good donor ligand PMe_3, generating an extremely electron rich all-alkylphosphine ruthenium(0) complex with the formula $Ru(DMPE)_2(PMe_3)$. Chatt had postulated the formation of $Ru(DMPE)_2(PEt_3)$ on the basis of the observation of free naphthalene upon treating $Ru(DMPE)_2(nap)H$ with PEt_3.[2] Only two other such complexes with iron(0) have been isolated, one by Karsch, $Fe(PMe_3)_3(Me_2PCH_2PMe_2)$,[8] and one by Ittel, Tolman, English, and Jesson, $Fe(DMPE)_2(PEt_3)$.[9] The related pentakis(trialkyl phosphite) complexes of Fe(0) and Ru(0) have been prepared and found to be fluxional molecules with a trigonal-bipyramidal structure.[10] Mixed derivatives such as $Ru(DMPE)_2[P(OMe)_3]$[11] and $Ru(PMe_3)_2[P(OMe)_3]_3$[12] are also known. Theoretical studies of the class of ML_5 systems with a d^8 configuration have been put forth.[13] The structures and substitution reactions of the PMe_3 and CO derivatives of the Chatt-type molecules $Ru(DMPE)_2L$ are compared in this report.

Results

The complex $Ru(DMPE)_2(nap)H$ was prepared by the reaction of 2 equiv of sodium naphthalenide with $Ru(DMPE)_2Cl_2$ in THF solution.[2] The isolated naphthyl hydride complex was then treated with a 10-fold excess of trimethylphosphine (0.46 M) and heated to 60 °C in benzene-d_6 or THF solution. A reaction slowly occurred that could be conveniently monitored by ^1H NMR spectroscopy, producing naphthalene (δ 7.618, dd, J = 6.1, 3.3 Hz, 4 H; δ 7.241, dd) and the new extremely air-sensitive orange complex **1**. Complex **1** was identified as the new zerovalent ruthenium derivative $Ru(DMPE)_2(PMe_3)$ on the basis of its ^1H NMR spectrum (C_6D_6): δ 1.128 (d, J = 3.9 Hz, 9 H); 1.413, 1.394 (28 H combined); 1.571 (br s, 4 H). No reaction is observed between $Ru(DMPE)_2(nap)H$ and tri-*tert*-butylphosphine at 60 °C after 24 h.

The ^{31}P NMR spectrum of **1** showed a large doublet at δ 38.63 (J = 5.5 Hz) and a broad multiplet at δ 35.85 of lesser intensity as expected for a molecule with two distinct types of phosphorous atoms. The spectrum was invariant down to −100 °C in toluene solution.

While the large doublet in the ^{31}P NMR spectrum of **1** suggests a square-pyramidal structure, the ^1H NMR data are consistent with either a fluxional trigonal-bipyramidal or static square-pyramidal structure. Since there are no known square-pyramidal pentakis(phosphine) or -(phosphite) complexes, an X-ray structural determination of **1** was made by growing orange crystalline needles from hexane solution. X-ray examination of a dozen crystals on a CAD-4 diffractometer revealed one sample that was suitable for further data collection on the basis of the high quality of the unit cell parameters determined from 25 reflections. An orthorhombic cell was determined with absences consistent with the space groups $Pna2_1$ and *Pnam* (conventional setting, *Pnma*). A reasonable density (d_{calcd} = 1.3 g/cm^3) indicated Z = 4, which corresponds to a general position for the ruthenium atom in $Pna2_1$ or a special position in *Pnam*. Standard data collection proceeded smoothly with 0.8% change in intensity of three standard reflections.

Refinement was first attempted in space group *Pnam*. A Patterson map solution revealed the Ru position on a mirror plane (z = 0.25). Refinement of the metal position and isotropic B parameter allowed the location of three unique phosphorus atoms on a difference Fourier map. One phosphorus (P1) was located on the mirror plane (z = 0.25) and was therefore assigned as the PMe_3 phosphorus. The remaining two phosphorus atoms were assigned as P2 and P3 of the DMPE ligand set. Further refinement of the four heavy atoms was carried out first isotropically and then anisotropically. A difference Fourier map revealed several peaks within bonding distance to each phosphorus (1.7 Å < d_{Ru-P} < 2.0 Å) of intensity less than that for a carbon atom (1–2 e/Å^3) with Ru–P–C and C–P–C bond angles of 95–115°, consistent with disorder of the DMPE ligand between two geometries rotated by 90° about the Ru–P1 vector.

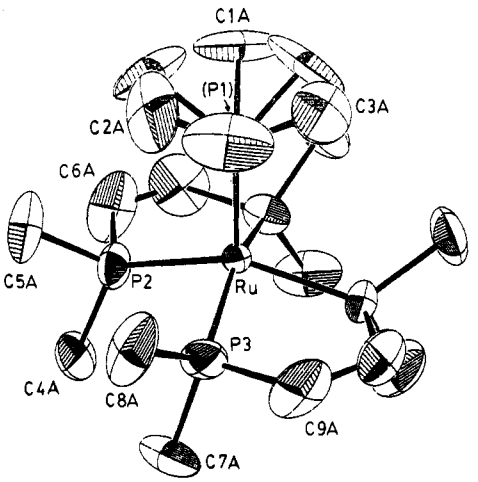

Figure 1. ORTEP drawing of $Ru(DMPE)_2(PMe_3)$. Ellipsoids are shown at the 30% probability level.

In addition, three peaks appeared for the carbon atoms attached to P1 with intensities about half that for a carbon atom (1–2 e/Å^3). These peaks generate a second set of three carbon atoms due to the mirror plane and were identified as being associated with a 180° rotational disorder of the PMe_3 group about the Ru–P1 axis. These two disorders were successfully refined as outlined below.

One group of six DMPE carbon atoms attached to P2 and P3 (three associated with each half of two separate DMPE ligands) could be picked out as a contributor to one conformation (A) from the difference Fourier map. Isotropic refinement of the six carbon atoms was carried out first with populations of 50%, after which a second group of six DMPE carbons (B) with the methylene bridges spanning P2 and P3 were refined isotropically (also with 50% populations).

Next, the three carbon atoms attached to P1 were introduced and refined isotropically. Final structure refinement was carried out by cyclic variation of the RuP_3 unit along with one of three separate groups of carbon atoms, the latter comprised of the $(DMPE)_A$, $(DMPE)_B$, or PMe_3 ligand. Convergence ultimately occurred with R_1 = 0.042, R_2 = 0.066, and a goodness of fit of 2.39. The location of the Ru and P1 atoms on the mirror plane and the mirror relationship between the halves of the DMPE ligands confirmed *Pnam* as the proper space group. Note that *Pnam* is a special case of $Pna2_1$ in which the molecule also possesses or is related by a mirror plane perpendicular to the z axis in addition to the *n*-glide, *a*-glide, and 2_1 screw axis.

An ORTEP drawing of the conformer is shown in Figure 1, displaying the rotational disorder about *P*1 but only one of two DMPE configurations. Bond distances and angles are given in Table I, and atomic coordinates are given in Table II, although the approximation made by using a single phosphorus atom for both of the 0.5-occupancy phosphorus atoms of the disordered DMPE ligand dictates larger real errors in the bond distances and angles. Disorder of coordinated DMPE has been observed in $Ru(DMPE)_2(nap)H$,[14] although not due to an apparent C_4 axis.

The rate of reaction of $Ru(DMPE)_2(nap)H$ (0.048 M) with PMe_3 (0.09 M) in C_6D_6 was monitored at 25 °C. Slow reaction occurred over several weeks and was observed to follow first-order

(8) Karsch, H. H. *Angew. Chem., Int. Ed. Engl.* **1982**, *21*, 311–312.
(9) Ittel, S. D.; Tolman, C. A.; English, A. D.; Jesson, J. P. *J. Am. Chem. Soc.* **1976**, *98*, 6073–6075.
(10) Muetterties, E. L.; Rathke, E. L. *J. Chem. Soc., Chem. Commun.* **1974**, 850–851. English, A. D.; Ittel, S. D.; Tolman, C. A.; Meakin, P.; Jesson, J. P. *J. Am. Chem. Soc.* **1977**, *99*, 117–120.
(11) Tolman, C. A.; Ittel, S. D.; English, A. D.; Jesson, J. P. *J. Am. Chem. Soc.* **1978**, *100*, 4080–4089.
(12) Werner, H.; Gotzig, J. *J. Organomet. Chem.* **1985**, *284*, 73–93.
(13) Rossi, A. R.; Hoffmann, R. *Inorg. Chem.* **1975**, *14*, 365–374.
(14) Cf.: Gregory, U. A.; Ibekwe, S. D.; Kilborn, B. T.; Russell, D. R. *J. Chem. Soc. A* **1971**, 1118–1125.

Table I. Distances (Å) and Angles (deg) in $Ru(DMPE)_2(PMe)_3$

Ru–P1	2.297 (1)	P3–C9A	1.918 (10)
Ru–P2	2.268 (1)	P2–C4B	1.860 (11)
Ru–P3	2.268 (1)	P2–C5B	1.724 (11)
P1–C1A	1.819 (11)	P2–C6B	1.887 (14)
P1–C2A	1.742 (12)	P3–C7B	1.843 (10)
P1–C3A	1.797 (11)	P3–C8B	1.67 (2)
P2–C4A	1.825 (11)	P3–C9B	1.864 (12)
P2–C5A	1.849 (11)	C6A–C6A′	1.40 (3)
P2–C6A	1.900 (11)	C9A–C9A′	1.56 (2)
P3–C7A	1.830 (13)	C6B–C9B	1.55 (2)
P3–C8A	1.852 (10)		
P1–Ru–P2	103.69 (4)	Ru–P2–C6A	108.1 (4)
P1–Ru–P3	103.49 (5)	Ru–P2–C4B	126.7 (4)
P2–Ru–P2′	86.38 (7)	Ru–P2–C5B	126.2 (5)
P3–Ru–P3′	86.00 (6)	Ru–P2–C6B	108.2 (5)
P2–Ru–P3	87.48 (5)	C7A–P3–C8A	100.0 (7)
P2–Ru–P3′	152.82 (5)	C7A–P3–C9A	103.4 (6)
Ru–P1–C1	120.1 (4)	C8A–P3–C9A	93.5 (5)
Ru–P1–C2	123.7 (6)	C7B–P3–C8B	102.4 (7)
Ru–P1–C3	122.1 (5)	C7B–P3–C9B	89.8 (6)
C1A–P1–C2A	93.0 (9)	C8B–P3–C9B	86.9 (9)
C1A–P1–C3A	91.0 (7)	Ru–P3–C7A	122.2 (5)
C2A–P1–C3A	98.9 (9)	Ru–P3–C8A	123.6 (4)
C4A–P2–C5A	98.8 (7)	Ru–P3–C9A	108.9 (3)
C4A–P2–C6A	103.3 (7)	Ru–P3–C7B	122.2 (4)
C5A–P2–C6A	99.3 (6)	Ru–P3–C8B	130.8 (6)
C4B–P2–C5B	101.0 (7)	Ru–P3–C9B	110.8 (5)
C4B–P2–C6B	93.7 (7)	P2–C6A–C6A	116.7 (4)
C5B–P2–C6B	89.7 (8)	P3–C9A–C9A	113.6 (3)
Ru–P2–C4A	121.1 (4)	P2–C6B–C9B	117.6 (8)
Ru–P2–C5A	122.8 (4)	P3–C9B–C6B	112.0 (8)

Table II. Positional Parameters for $Ru(DMPE)_2(PMe_3)$

atom	*x*	*y*	*z*
Ru	0.10709 (3)	0.11609 (5)	0.250
P1	−0.0149 (1)	−0.0061 (3)	0.250
P2	0.1830 (1)	−0.0010 (2)	0.3469 (1)
P3	0.0875 (1)	0.2907 (2)	0.3466 (1)
C1A	−0.0231 (9)	−0.178 (2)	0.197 (1)
C2A	−0.062 (1)	−0.070 (3)	0.340 (1)
C3A	−0.1037 (7)	0.060 (2)	0.196 (1)
C4A	0.267 (1)	0.089 (2)	0.401 (1)
C5A	0.137 (1)	−0.097 (2)	0.437 (1)
C6A	0.2356 (9)	−0.158 (2)	0.294 (1)
C7A	0.173 (1)	0.390 (2)	0.393 (1)
C8A	0.021 (1)	0.270 (2)	0.4391 (8)
C9A	0.021 (1)	0.439 (1)	0.299 (1)
C4B	0.296 (1)	0.005 (2)	0.359 (1)
C5B	0.162 (2)	−0.167 (2)	0.390 (1)
C6B	0.163 (2)	0.085 (2)	0.4517 (8)
C7B	0.161 (1)	0.438 (1)	0.3622 (8)
C8B	0.002 (2)	0.359 (3)	0.386 (2)
C9B	0.110 (2)	0.223 (2)	0.4536 (8)

kinetics with $k_{obsd} = 1.5 \times 10^{-7}$ s^{-1}. Bimolecular substitution would have been revealed by curvature of the ln (% $[Ru(DMPE)_2(nap)H]$) vs. time plot after 1–2 half-lives, but no such curvature was found. There was no evidence for formation of $Ru(DMPE)_2(C_6D_5)D$ during the reaction.

Compound **1** reacts with a variety of ligands upon standing at 23 °C in benzene solution. Under an atmosphere of CO, ^{1}H NMR resonances for free PMe_3 are observed to grow in rapidly (δ 0.78, d, J = 2.4 Hz) as resonances for **1** disappear. A new broad singlet appears at δ 1.311. These changes can be interpreted in terms of the formation of the pale yellow carbonyl complex $Ru(DMPE)_2(CO)$ (**2**) as PMe_3 is lost (eq 3). The latter species is

$$\underset{\mathbf{1}}{Ru(DMPE)_2(PMe_3)} + CO \xrightarrow{k_2} \underset{\mathbf{2}}{Ru(DMPE)_2(CO)} + PMe_3 \quad (3)$$

found to have ν_{CO} 1945 cm^{-1}, the low frequency being consistent with bonding to an electron-rich ruthenium center.

The kinetics of reaction 3 in benzene solution was investigated as a function of the CO pressure above the solution by monitoring

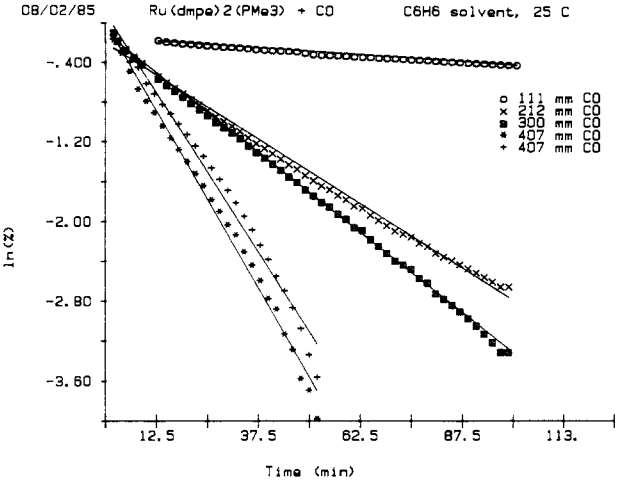

Figure 2. Effect of CO pressure upon the rate of substitution in **1**.

Table III. Effect of CO Pressure on the Rate of Exchange with **1**

P_{CO}, mm	k_{obsd}, s^{-1}	k_2, atm^{-1} s^{-1}
111	4.5×10^{-5}	3.1×10^{-4}
212	4.7×10^{-4}	1.7×10^{-3}
300	5.3×10^{-4}	1.3×10^{-3}
407	1.2×10^{-3}	2.2×10^{-3}
407	1.1×10^{-3}	2.1×10^{-3}

the disappearance of **1** by UV–vis spectroscopy at 280 nm and plotting the absorbance according to eq 4. The observed rate

$$\ln\left(\frac{A_t - A_\infty}{A_0 - A_\infty}\right) = -k_{obsd}t = -k_2 P_{CO} t \quad (4)$$

constants obtained from the slope of these first-order plots were found to vary directly with the CO pressure over the range 100–400 mm CO (Figure 2, Table III). The rapidity of the reaction ($\tau_{1/2} \approx 15$ min) and the poor mixing of CO gas with the solution in the UV cell renders these experiments of limited value for determinining the value of the second-order rate constant k_2 in eq 3. The rate of reaction clearly increases with increasing CO pressure, however, indicating the participation of CO either in or prior to the rate-determining step.

Single-crystal X-ray analysis of this compound was carried out by growing crystals from ether–hexane solvent. Centering and refinement of 25 reflections revealed an orthorhombic crystal system with absences for the space group *Pbca*, with $d_{calcd} = 1.37$ g/cm^3 for $Z = 16$. In this space group a molecule in a general position is only 8-fold degenerate, implying that there were two crystallographically independent molecules in the asymmetric unit. Data collection and reduction followed by direct-methods (MULTAN) solution of the structure revealed the position of the ruthenium atoms. Subsequent cycles of difference Fourier maps and least-squares refinement showed all non-hydrogen atoms. Anisotropic refinement converged with $R_1 = 0.048$ and $R_2 = 0.066$. An ORTEP drawing of one of the two independent molecules is shown in Figure 3. Distances and angles are given in Table IV and atomic coordinates in Table V.

The CO adduct **2** does not react reversibly with PMe_3 upon heating to 60 °C. Treatment of **2** with high concentrations (8 M) of PMe_3 (in excess) in a sealed NMR tube does not result in any detectable formation of **1**.

The exchange of PMe_3 in **1** with added $P(CD_3)_3$ was examined by monitoring the appearance of free PMe_3 relative to coordinated PMe_3 in **1** by ^{1}H NMR spectroscopy. Reaction of **1** with excess $P(CD_3)_3$ was observed to follow good first-order kinetics as revealed by logarithmic plots of the percent completion vs. time according to eq 5, in which k_{obsd} represents the rate of approach

$$\ln\left(\frac{(\%\text{ of }\mathbf{1}\text{ at equil}) - (\%\text{ of }\mathbf{1}\text{-}d_9)}{100 - (\%\text{ of }\mathbf{1}\text{ at equil})}\right) = -k_{obsd}t \quad (5)$$

to equilibrium. Variation of $[P(CD_3)_3]$ over the range 0.25–0.62

Table IV. Selected Distances (Å) and Angles (deg) in Ru(DMPE)$_2$(CO)

First of Two Independent Molecules			
Ru–P1	2.284 (2)	Ru–P4	2.305 (2)
Ru–P2	2.300 (2)	Ru–C1	1.883 (9)
Ru–P3	2.299 (2)		
P1–Ru–P2	83.67 (8)	P2–Ru–P4	111.32 (8)
P1–Ru–P3	178.16 (8)	P2–Ru–C1	124.3 (2)
P1–Ru–P4	97.58 (8)	P3–Ru–P4	83.23 (8)
P1–Ru–C1	88.8 (2)	P3–Ru–C1	89.3 (2)
P2–Ru–P3	97.59 (8)	P4–Ru–C1	124.4 (2)
Second of Two Independent Molecules			
Ru′–P1′	2.295 (2)	Ru′–P4′	2.303 (2)
Ru′–P2′	2.301 (2)	Ru′–C1′	1.816 (10)
Ru′–P3′	2.289 (2)		
P1′–Ru′–P2′	83.67 (8)	P2′–Ru′–P4′	111.32 (8)
P1′–Ru′–P3′	178.16 (8)	P2′–Ru′–C1′	124.3 (2)
P1′–Ru′–P4′	97.58 (8)	P3′–Ru′–P4′	83.23 (8)
P1′–Ru′–C1′	88.8 (2)	P3′–Ru′–C1′	89.3 (2)
P2′–Ru′–P3′	97.59 (8)	P4′–Ru′–C1′	124.4 (2)

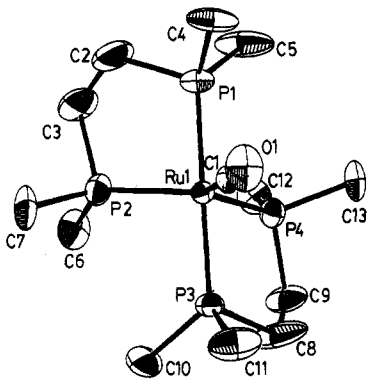

Figure 3. ORTEP drawing of Ru(DMPE)$_2$(CO). Ellipsoids are shown at the 30% probability level.

M showed only experimental scatter of k_{obsd} vs. [P(CD$_3$)$_3$] for six runs (Table VI). While the individual experiments provide good first-order behavior, the extreme air sensitivity of **1** combined with accurate measurement of [P(CD$_3$)$_3$] introduced variations from run to run. It is clear, however, that the rate of phosphine exchange ($\tau_{1/2} \approx 1500$ min) is much slower than the rate of CO exchange ($\tau_{1/2} \approx 15$ min).

Thermolysis of **1** at 23 °C in the presence of 1 equiv of neopentyl isocyanide (0.074 M) resulted in a very slow substitution reaction ($\tau_{1/2} \approx 2500$ min, eq 6). Heating the solution to 40 °C

$$\underset{\mathbf{1}}{\text{Ru(DMPE)}_2(\text{PMe}_3)} + \text{CNR} \rightarrow \text{Ru(DMPE)}_2(\text{CNR}) + \text{PMe}_3 \quad (6)$$

slowly produces the complex Ru(DMPE)$_2$(CNCH$_2$CMe$_3$) in 90% yield after 48 h. The ^{1}H NMR spectrum of this complex shows a broad singlet at δ 1.330 (~32 H) for the coordinated DMPE and singlets at δ 3.257 (2 H) and 1.078 (9 H) for the coordinated neopentyl isocyanide. An IR spectrum in hexane displays strong bands for $\nu_{C\equiv N}$ at 1770 cm^{-1} and ν_{C-N} at 930 cm^{-1}.

Discussion

The complex Ru(DMPE)$_2$(nap)H is known to lose naphthalene upon heating to 60 °C.[3] The results presented here indicate that the coordinatively unsaturated intermediate [Ru(DMPE)$_2$] can be trapped by small-cone-angle alkylphosphines to generate the zerovalent 18-electron species, even in benzene solvent. Trimethylphosphine, with a cone angle of 118°, is able to form a stable complex whereas tri-*tert*-butylphosphine, with a cone angle of 182°, is too large to coordinate to the metal.[15] The observation of formation of a trimethylphosphine complex in benzene solvent is also somewhat surprising in that while arene activation by [Ru(DMPE)$_2$] has been widely observed previously, no solvent activation is seen here despite the large excess of solvent (130:1 C$_6$D$_6$:PMe$_3$). The kinetics of substitution of PMe$_3$ for naphthalene are first order, ruling out a possible bimolecular displacement of naphthalene in an η^2-naphthalene intermediate by PMe$_3$ (eq 7).

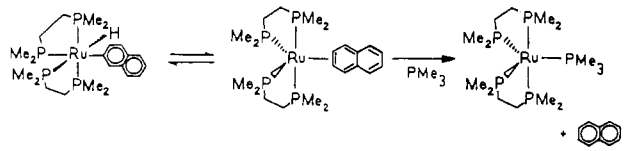

(7)

Thermolysis of **1** at 25 °C in the presence of a good ligand for ruthenium(0) such as CO results in the formation of the complex Ru(DMPE)$_2$(CO). Formation of the latter product occurs with a half-life of ~15 min at 25 °C, suggesting that the phosphine is quite labile compared to naphthalene. Since complex **1** is coordinatively saturated, all chemistry might be expected to occur by way of initial dissociation of phosphine to generate the same 16-electron intermediate that is formed upon thermolysis of Ru(DMPE)$_2$(nap)H.

The difference in the rates for CO, P(CD$_3$)$_3$, and CNR substitution suggested that PMe$_3$ dissociation was not rate-limiting, however. The rate of exchange of coordinated PMe$_3$ with added P(CD$_3$)$_3$ represents the maximum possible rate of PMe$_3$ dissociation from **1**. Since CO exchange with **1** occurs at least 100

Table V. Positional Parameters for Ru(DMPE)$_2$(CO)

atom	x	y	z
Ru1	0.17253 (4)	0.03297 (3)	0.70540 (4)
Ru1′	0.03578 (4)	0.75131 (4)	0.05961 (4)
P1	0.2372 (2)	0.0011 (1)	0.7998 (2)
P1′	0.1293 (2)	0.7534 (1)	−0.0171 (2)
P2	0.2448 (2)	−0.0270 (1)	0.6409 (2)
P2′	0.1161 (2)	0.7887 (1)	0.1385 (2)
P3	0.1078 (2)	0.0680 (1)	0.6116 (2)
P3′	−0.0594 (2)	0.7470 (2)	0.1335 (2)
P4	0.0692 (2)	−0.0127 (1)	0.7345 (2)
P4′	−0.0266 (2)	0.8240 (1)	0.0047 (2)
O1	0.2114 (4)	0.1566 (3)	0.7468 (5)
O1′	0.0302 (4)	0.6214 (3)	0.0418 (5)
C1	0.1951 (5)	0.1095 (5)	0.7311 (5)
C1′	0.0308 (5)	0.6715 (5)	0.0488 (5)
C2	0.3153 (7)	−0.0387 (7)	0.7687 (9)
C2′	0.2113 (6)	0.7618 (6)	0.0305 (8)
C3	0.3047 (8)	−0.0666 (7)	0.7037 (8)
C3′	0.2010 (6)	0.8054 (6)	0.0920 (8)
C4	0.2847 (7)	0.0526 (5)	0.8557 (6)
C4′	0.1533 (7)	0.6895 (6)	−0.0699 (7)
C5	0.1989 (8)	−0.0442 (6)	0.8691 (7)
C5′	0.1492 (7)	0.7413 (6)	0.2116 (7)
C6	0.2148 (7)	−0.0885 (5)	0.5858 (7)
C6′	0.1067 (6)	0.8575 (5)	0.1884 (7)
C7	0.3109 (6)	0.0038 (6)	0.5799 (7)
C7′	0.1353 (9)	0.8090 (6)	−0.0869 (8)
C8	0.0144 (7)	0.0535 (7)	0.6268 (8)
C8′	−0.1280 (7)	0.7974 (8)	0.1060 (8)
C9	0.0015 (6)	0.0027 (7)	0.6644 (7)
C9′	−0.1090 (8)	0.8372 (7)	0.058 (1)
C10	0.1185 (8)	0.0445 (7)	0.5194 (7)
C10′	−0.1085 (7)	0.6768 (7)	0.1351 (9)
C11	0.1025 (8)	0.1457 (5)	0.5975 (8)
C11′	−0.0507 (7)	0.7620 (7)	0.2291 (6)
C12	0.0574 (6)	−0.0924 (5)	0.7402 (7)
C12′	−0.0644 (9)	0.8120 (7)	−0.0851 (7)
C13	0.0224 (6)	0.0110 (6)	0.8185 (6)
C13′	0.0007 (8)	0.9006 (5)	−0.0017 (7)

Table VI. Effect of P(CD$_3$)$_3$ Concentration on Rate of Exchange with **1**

[P(CD$_3$)$_3$], M	k_{obsd}, s^{-1}	[P(CD$_3$)$_3$], M	k_{obsd}, s^{-1}
0.24	9.0×10^{-6}	0.37	5.6×10^{-6}
0.25	7.2×10^{-6}	0.46	5.6×10^{-6}
0.36	8.9×10^{-6}	0.62	1.2×10^{-5}

(15) Tolman, C. *Chem. Rev.* **1977**, *77*, 313–333.

Scheme I

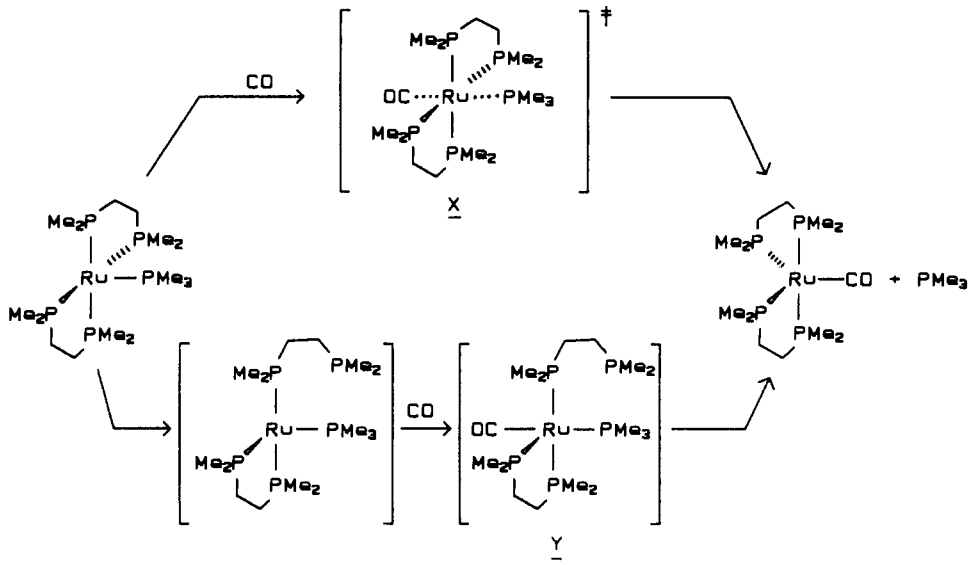

times faster, the exchange must occur *without* prior PMe_3 dissociation, i.e., by an associative process. The dependence of the rate upon CO pressure experimentally verifies the bimolecular nature of this substitution.

The exchange of $P(CD_3)_3$ and $CNCH_2CMe_3$ in **1** is consistent with a reversible preequilibrium involving PMe_3 dissociation, followed by trapping by the incoming ligand (eq 8). This

$$Ru(DMPE)_2(PMe_3) \underset{k_{-1}}{\overset{k_1}{\rightleftharpoons}} [Ru(DMPE)_2] \xrightarrow[k_2]{L} Ru(DMPE)_2(L) \quad (8)$$

$$L = P(CD_3)_3,\ CNCH_2CMe_3$$

mechanism requires that the rate of labeled $P(CD_3)_3$ exchange correspond to k_1 ($k_{-1} = k_2$) as the rate-determining step. The slower exchange of isocyanide indicates that k_2 is rate-limiting for CNR substitution. The trapping of $[Ru(DMPE)_2]$ by PMe_3 ($k_{-1}[PMe_3]$) must exceed the rate of reaction with CNR ($k_2[CNR]$) in accord with the slower exchange of CNR compared with that of $P(CD_3)_3$.

Two separate pathways can be proposed to accommodate the associative mechanism for CO substitution. The first of these involves a direct displacement of coordinated PMe_3 by attack of the CO at the vacant site of the base of the square pyramid. This mechanism involves an "S_N2-like" transition state in which the entering ligand fills out an octahedral coordination site in the transition state (X, Scheme I). This mechanism might also be termed an associative-interchange (I_a) reaction.

A second possible mechanism involves a reversible dissociation of one end of the DMPE ligand followed by rate-determining coodination of CO and rapid dissociation of PMe_3 (Scheme I). Both mechanisms have the same kinetic form (as long as the DMPE preequilibrium is faster than CO trapping) and cannot be distinguished between by these studies. The intermediate Y in Scheme I might exclusively lose PMe_3 and not the more bulky ligand DMPE if the trans-labilizing effect of CO exceeds that of DMPE. Labilization of one end of a chelating ligand in substitution reactions of chelating amines and phosphines has also been observed by Dobson.[16]

The present investigation indicates a new structure for the zerovalent alkylphosphine derivative $Ru(DMPE)_2(PMe_3)$. In the square-pyramidal geometry, the ruthenium was found to lie slightly above the plane of the four DMPE phosphorus atoms (0.53 Å) with a P1–Ru–(basal P) ligand angle of 103.6° (average). The observed geometry is substantially different from that expected for a trigonal-bipyramid structure, in which two of the phosphorus atoms would be expected to assume a trans disposition around the ruthenium atom. Furthermore, a Berry-type distortion would be expected for a molecule between these two limiting geometries, but no such distortion is seen. The observation of a square-pyramidal structure for a five-coordinate d^8 complex was not anticipated, as most compounds of this class are found to be trigonal bipyramidal.[17] d^8 five-coordinate molecules known to adopt a square-pyramidal structure include $Ni(CN)_5^{3-}$,[18] $Ni(2\text{-MeIm})_4Br^+$, and $NiCl_2Cl'(2,9\text{-}Me_2phen)$[19] (Im = imidazole, phen = phenanthroline), but no pentakis(phosphine) or -(phosphite) complexes are known to have this geometry.

In contrast, the structure of the carbonyl adduct was found to have a trigonal-bipyramidal structure, in accord with other five-coordinate d^8 iron and ruthenium complexes. The two crystallographically independent molecules show virtually identical geometries with respect to the ruthenium and two DMPE phosphine ligands, but the equatorial CO is bent toward one of the equatorial phosphines such that it no longer lies along the angle bisector of the equatorial P2′–Ru′–P4′ unit. The other distortion displayed by the first molecule is that the axial P1–Ru–P3 vector is not perfectly normal to the equatorial plane but lies at an angle of 86° minimum in the direction of C1.

Hoffmann has summarized the orbital approach to trigonal-bipyramidal vs. square-pyramidal coordination in five-coordinate complexes.[13] While his analysis does not predict which geometry is prefered, it does indicate that for d^8 complexes a π-acceptor ligand is preferred in the equatorial position of a trigonal-bipyramidal molecule.

Finally, the number of coordinatively saturated organometallic molecules known to undergo associative substitution is quite small. Those that do often have ligands such as η^5-C_5H_5, indenyl, NO, and allyl, which are all capable of intramolecularly providing a vacant site for the incoming ligand,[21] thereby avoiding a 20-electron intermediate or transition state. Some octahedral coordination compounds such as $[Cr(H_2O)_6]^{3+}$ show a large de-

(16) Dobson, G. R.; Binzet, N. S. *J. Coord. Chem.* **1984**, *13*, 153–157. Dobson, G. R.; Mansour, S. E.; Halverson, D. E.; Erikson, E. S. *J. Am. Chem. Soc.* **1983**, *105*, 5505–5506. Dobson, G. R.; Dobson, C. B.; Halverson, D. E.; Mansour, S. E. *J. Organomet. Chem.* **1983**, *253*, C27–C32.

(17) Muetterties, E. L. *Acc. Chem. Res.* **1970**, *3*, 266–273.

(18) Raymond, K. N.; Coefield, P. W. R.; Ibers, J. A. *Inorg. Chem.* **1968**, *7*, 1362–1372.

(19) Wood, J. S. *Prog. Inorg. Chem.* **1972**, *16*, 227–486.

(20) *Organic Syntheses*; Baumgarten, H. E., Ed.; Wiley: New York, 1973; Collect. Vol. 5, p 1060.

(21) See, for examples: (a) Hart-Davis, A. J.; Mawby, R. J. *J. Chem. Soc. A* **1969**, 2403. (b) Ji, L. N.; Rerek, M. E.; Basolo, F. *Organometallics* **1984**, *3*, 740–745. (c) Casey, C. P.; Jones, W. D. *J. Am. Chem. Soc.* **1980**, *102*, 6154–6156. (d) Casey, C. P.; Jones, W. D.; Harsey, S. G. *J. Organomet. Chem.* **1981**, *206*, C38–C42. (e) Casey, C. P.; O'Conner, J. W.; Jones, W. D.; Haller, K. *Organometallics* **1983**, *2*, 535–538.

pendence of rate of anation on the entering ligand, implying an I_a mechanism, although this path is far less common than either the I_d or purely dissociative mechanism.[22] As mentioned earlier, Dobson has also provided evidence for associative substitution by labilization of one end of a chelating ligand.[16] The ability of **1** to undergo associative CO substitution may be related to the square-pyramidal geometry, which maintains a sterically vacant position for S_N2 attack by CO.

Conclusion

It is possible to prepare pentacoordinate alkylphosphine complexes of ruthenium(0), provided the ligand cone angles permit coordination. The d^8 complex $Ru(DMPE)_2(PMe_3)$ is found to have square-pyramidal geometry, whereas the carbonyl complex prefers trigonal-bipyramidal geometry. The trimethylphosphine complex undergoes associative substitution with CO but dissociative substitution with other larger ligands.

Experimental Section

All solvents were distilled from dark purple solutions of sodium benzophenone ketyl under a nitrogen atmosphere. All compounds were handled in a Vacuum Atmospheres Dri-Lab. All experiments were performed in sealed NMR tubes or ampules prepared and degassed on a high-vacuum line. Neopentyl isocyanide was prepared by the method of Ugi.[20] $Ru(DMPE)_2(nap)H$ was prepared according to the literature method.[2]

High-field ^1H NMR (400.13 MHz) spectra were recorded on a Bruker WH-400 NMR spectrometer. Temperature for the NMR experiments was regulated by a Bruker BVT-1000 temperature control unit (±0.1 °C). Calibration was determined by plotting the separation of the two resonances of a standard methanol sample vs. the Pt sensor voltage of the BVT-1000 unit. X-ray structural investigations were carried out on an Enraf-Nonius CAD-4 diffractometer coupled to a TEXRAY PDP-11 computer. UV–vis spectra were recorded on a Perkin-Elmer 330 spectrometer fitted with a temperature-controlled cell holder attached to a Brinkman/Lauda recirculating bath.

Preparation of $Ru(DMPE)_2(PMe_3)$ (1). $Ru(DMPE)_2(nap)H$ (250 mg, 0.47 mmol) was introduced into a reaction tube attached to a ground-glass joint and PMe_3 (4.7 mmol) plus THF (5 mL) distilled into the tube (25 °C, 10^{-4} mm). The tube was sealed under vacuum and heated to 50 °C for 10 days. The solvent was removed (25 °C, 10^{-4} mm) and the naphthalene sublimed away from the product at 40 °C (10^{-4} mm). Recrystallization from hexane afforded $Ru(DMPE)_2(PMe_3)$ in 71% isolated yield (160 mg). ^1H NMR (C_6D_6): δ 1.128 (d, J = 3.9 Hz, 9 H); 1.413, 1.394 (28 H combined); 1.571 (br s, 4 H).

Reaction of $Ru(DMPE)_2(PMe_3)$ (1) with CO. A benzene-d_6 solution of **1** (20 mg, 0.040 mmol, in 0.5 mL) was sealed in a 5-mm NMR tube under 350 mm of CO on the vacuum line. A ^1H NMR spectrum recorded after 10 min showed resonances for free PMe_3 and a new product displaying a large broad singlet at δ 1.31, assigned to $Ru(DMPE)_2(CO)$. Removal of the solvent afforded the product in quantitative yield. IR (KBr): 2958 (w), 2905 (w), 1945 (s), 1925 (sh), 1453 (sh), 1429 (m), 1380 (m), 1300 (m), 942 (s), 910 (m), 860 (w), 724 (m) cm^{-1}.

Reaction of $Ru(DMPE)_2(PMe_3)$ (1) with Neopentyl Isocyanide. A benene solution (0.5 mL) of **1** (18 mg, 0.037 mmol) and neopentyl isocyanide (3.6 mg, 0.037 mmol) were placed in an NMR tube attached to a ground-glass joint. The solution was freeze–pump–thaw-degassed on the vacuum line and sealed under vacuum. The light yellow solution was allowed to react at 23 °C for 19 h and then heated to 40 °C for 48 h. The extent of reaction was monitored by ^1H NMR spectroscopy by following the disappearance of the starting material and $CNCH_2CMe_3$ resonances as those of the product and PMe_3 appeared. Removal of the solvent at 25 °C (10^{-4} mm) yielded 16 mg (85%) of the product $Ru(DMPE)_2(CNCH_2CMe_3)$. ^1H NMR (C_6D_6): δ 1.08 (s, 9 H); 1.33 (br s, 32 H); 3.25 (s, 2 H). IR (hexane): 1770 (vs), 1413 (w), 1375 (sh), 1327 (w), 1285 (w), 1271 (w), 930 (s), 882 (m), 870 (m), 830 (w), 700 (m), 685 (m), 640 (w) cm^{-1}.

Kinetics of the Reaction of $Ru(DMPE)_2(nap)H$ with PMe_3. $Ru(DMPE)_2(nap)H$ (10 mg, 0.019 mmol) was weighed into an NMR tube attached to a ground-glass joint and PMe_3 (0.036 mmol) plus 0.4 mL of C_6D_6 distilled into the tube (25 °C, 10^{-4} mm). The tube was sealed under vacuum and allowed to react in the dark at 25 °C for 18 weeks. During this period, the disappearance of resonances in the ^1H NMR spectrum for the starting complex gave way to new resonances for the product **1** and free naphthalene. The extent of reaction was monitored by integration of the ratio of free (δ 0.788) to coordinated (δ 1.128) PMe_3.

Table VII. Summary of Crystallographic Data[a]

	$Ru(DMPE)_2(PMe_3)$	$Ru(DMPE)_2(CO)$
Crystal Parameters		
formula	$RuP_5C_{15}H_{41}$	$RuP_4OC_{13}H_{32}$
fw	477.434	429.37
cryst syst	orthorhombic	orthorhombic
space group	*Pnam*	*Pbca*
Z	4	16
a, Å	16.3540 (18)	19.110 (9)
b, Å	9.3240 (30)	23.116 (6)
c, Å	16.0210 (23)	18.780 (6)
vol, Å^3	2443.0 (1.4)	8296.1
d_{calcd}, g/cm^3	1.298	1.375
cryst dimens, mm	0.22 × 0.13 × 0.18	0.56 × 0.34 × 0.19
temp. °C	23	23
Measurement of Intensity Data		
diffractometer	Enraf-Nonius CAD4, κ geometry	
radiation (monochromator)	Mo, 0.71073 Å (graphite)	
scan type	$2\theta/\omega$	
scan range, deg	0.7 + 0.35 tan θ	
scan rate, deg/min	1.2–20	
total bkgd time	(scan time)/2	
takeoff angle, deg	2.6	
2θ range, deg	4–45	4–46
data collected	$+h,+k,+l$	$+h,+k,+l$
no. of data collected	2229	5367
no. of unique data $>3\sigma$	1746	3387
no. of parameters varied		343
abs coeff, cm^{-1}	9.481	10.394
systematic absences	$0kl$, $k + l$ odd; $h0l$, h odd	$0kl$, k odd; $h0l$, l odd; $hk0$, h odd
R_1	0.042	0.048
R_2	0.066	0.066
goodness of fit	2.39	2.15

[a] Source of scattering factors f_0, f', f'': Cromer, D. T.; Waber, J. T. *International Tables for X-ray Crystallography*; Kynoch: Birmingham, England, 1974; Vol. IV, Tables 2.2B, 2.3.1.

Kinetics of the Reaction of $Ru(DMPE)_2(PMe_3)$ with $P(CD_3)_3$. $Ru(DMPE)_2(PMe_3)$ (5 mg) was weighed into an NMR tube attached to a ground-glass joint and C_6D_6 plus the required $P(CD_3)_3$ (see Table VI) distilled into the tube on a vacuum line. The tube was sealed and placed in the temperature-controlled (26.7 °C) probe of the NMR spectrometer. The disappearance of the PMe_3 doublet in **1** relative to the appearance of the resonance for free PMe_3 was used to monitor the percentage reaction during the approach to equilibrium. The percentage reaction at infinite time was calculated on the basis of the known amounts of **1** and $P(CD_3)_3$ originally placed in the sample tube and was used in eq 5 for determining the rate constant of the reaction.

Kinetics of the Reaction of $Ru(DMPE)_2(PMe_3)$ with CO. A solution of $Ru(DMPE)_2(PMe_3)$ in THF ($\sim 1 \times 10^{-3}$ M) was prepared and introduced in a 0.1 mm path length UV cell attached to a 5-mL reservoir bulb and Teflon stopcock. On the vacuum line, the solution in the bulb was cooled to −10 °C, the pressure of CO listed in Table III introduced, and the Teflon stopcock closed to isolate the sample bulb and cell from the vacuum line. After it was warmed to room temperature and shaken rapidly, the apparatus was tipped to fill the UV cell and the absorbance of the solution monitored at 280 nm in a thermostated cell holder (24 °C). The exponential decay of absorbance with time was fit to eq 4 in order to determine the rate constant for reaction. Unfortunately, the rate constants are close to the time required for sample mixing and temperature equilibration, reducing the accuracy of the constants. Absorbance data are shown in Figure 2.

X-ray Structural Determination of $Ru(DMPE)_2(PMe_3)$. Well-formed orange crystals of the compound were prepared by slow evaporation of a hexane solution. The lattice constants were obtained from 25 centered reflections with values of χ between 10 and 45°. Cell reduction with the program TRACER revealed only an orthorhombic crystal system. Data were collected on the crystal in accord with the parameters in Table VII. The Molecular Structure Corp. and Enraf-Nonius SDP programs were used for solution and refinement of the structure. The space group was determined to be either $Pna2_1$ or *Pnam* on the basis of the systematic absences ($0kl$, $k + l$ odd; $h0l$, h odd). Solution of the Patterson map revealed the ruthenium atom. Least-squares refinement (minimizing

(22) For a recent summary see: Atwood, J. D. *Inorganic and Organometallic Reaction Mechanisms*; Brooks/Cole: Monterey, CA, 1985.

$\sum w(|F_o| - |F_c|)^2$) of the ruthenium atom in space group *Pnam* followed by a difference Fourier map revealed three peaks for the DMPE and PMe_3 phosphorus atoms. Isotropic refinement of these atoms followed by anisotropic refinement converged with $R_1 = 0.113$, $R_2 = 0.179$.[23] A difference Fourier map showed several peaks within bonding distance to phosphorus (1.7-1.9 Å), indicating disorder for the DMPE and PMe_3 carbons.

A group of six DMPE carbon atoms attached to P2 and P3 (three associated with each half of two separate DMPE ligands, conformation A) could be picked out as a contributor to one conformation from the difference Fourier map. Refinement of the six carbon atoms was carried out by first holding the position of each atom fixed with a population of 50% and varying only the isotropic thermal parameters. The positions were subsequently allowed to vary also. A difference Fourier map now showed a second conformation of the six DMPE carbons with the methylene bridges spanning P2 and P3 (conformation B). These six carbons were also introduced with populations of 50% and their thermal parameters refined. The positions were then also allowed to vary.

Next, the three carbon atoms attached to C1 were introduced and refined first isotropically and then anisotropically. The two independent DMPE conformations were refined anisotropically in separate groups, with the RuP_3 parameters varied as well. Alternate refinement of the P1 methyl group, DMPE conformation A, and DMPE conformation B ultimately gave $R_1 = 0.042$ and $R_2 = 0.066$. Distances and angles are given in Table I, positional parameters are in Table II, and an ORTEP drawing is shown in Figure 1.

X-ray Structural Determination of $Ru(DMPE)_2(CO)$ (2). Well-formed colorless crystals of **2** were prepared by slow diffusion of a layered hexane-ether solution of **2**. The lattice constants were obtained from 25 centered reflections with values of χ between 10 and 45°. Cell reduction with the program TRACER revealed only an orthorhombic crystal system. Data were collected on the crystal in accord with the parameters in Table VII. The Molecular Structure Corp. and Enraf-Nonius SDP programs were used for solution and refinement of the structure. The space group was determined to be *Pbca* on the basis of the systematic absences (0*kl*, *k* odd; *h*0*l*, *l* odd; *hk*0, *h* odd). Solution was accomplished with the direct-methods program MULTAN due to the large number of Ru-Ru vectors in the Patterson map. Least-squares refinement of one of the ruthenium atoms and three of the phosphorus atoms followed by a difference Fourier map revealed the remaining ruthenium and all phosphorus atoms. Subsequent difference Fourier maps and least-squares refinements showed all DMPE carbons and the CO ligand with no evidence for disorder. Anisotropic refinement of all non-hydrogen atoms with a non-Poisson weighting scheme ($p = 0.04$) coverged with $R_1 = 0.048$, $R_2 = 0.066$,[23] GOF = 2.15. Table IV contains relevant bond distances and angles for one of the two molecules, and Table V gives positional parameters.

(23) $R_1 = \{\sum||F_o| - |F_c||\}/\{\sum|F_o|\}$ and $R_2 = \{\sum w(|F_o| - |F_c|)^2\}^{1/2}/\{\sum wF_o^2\}$, where $w = \{\sigma^2(F_o) + [pF_o^2]^2\}^{1/2}$ for the non-Poisson-contribution weighting scheme or $w = 1$ for unit weights.

Acknowledgment is made to the donors to the Petroleum Research Fund, administered by the American Chemical Society, to Research Corp., and to the U. S. Department of Energy (Grant No. 83ER13095) for their partial support of this work. W.D.J. also thanks the Camille and Henry Dreyfus Foundation for Young Faculty and Teacher-Scholar Awards. M.L. thanks the Italian CNR for financial support.

Registry No. **1**, 101519-28-2; **2**, 67409-67-0; $Ru(DMPE)_2(nap)H$, 24669-41-8; $Ru(DMPE)_2(CNCH_2CMe_3)$, 101519-29-3; PMe_3, 594-09-2; CO, 630-08-0.

Supplementary Material Available: A full ORTEP drawing of **1** and listings of anisotropic thermal parameters for **1** and **2** and bond distances and angles for **2** (7 pages). Ordering information is given on any current masthead page. According to policy instituted Jan 1, 1986, the tables of calculated and observed structure factors (52 pages) are being retained in the editorial office for a period of 1 year following the appearance of this work in print. Inquiries for copies of these materials should be directed to the Editor.

Contribution from the Department of Chemistry, Stanford University, Stanford, California 94305

A Binuclear Copper(II) Complex with a Bridging Thioether Ligand. Crystal and Molecular Structure of Dicopper Thiobis(ethylenenitrilo)tetraacetate Pentahydrate

Jeremy M. Berg and Keith O. Hodgson*

Received June 14, 1983

The copper(II) complex $Cu_2(TEDTA)\cdot 5H_2O$ (where TEDTA is the tetraanion of thiobis(ethylenenitrilo)tetraacetic acid) has been synthesized and its structure determined with use of X-ray diffraction methods. The crystals belong to the space group $P2_12_12_1$ with unit cell parameters $a = 9.646$ (4) Å, $b = 14.264$ (5) Å, $c = 14.724$ (5) Å, and $Z = 4$. The structure has been refined with use of full-matrix least squares to $R = 3.8\%$, $R_w = 4.7\%$. The crystal structure consists of binuclear units containing two independent Cu(II) ions, each in a tetragonally distorted octahedral environment. The thioether S atom bridges the Cu atoms. The crystal structure is held together by a combination of bridging carboxylate groups and an extended hydrogen-bond network.

Recent X-ray crystallographic studies of the blue copper proteins plastocyanin[1] and azurin[2] have revealed that the copper coordination sphere consists of a cysteinate sulfur, two nitrogens from histidine, and a thioether sulfur from methionine. Among the unanticipated features of this site is the strikingly long Cu-S(methionine) distance of 2.9 Å.[3] This Cu-S interaction is sufficiently long and weak that the sulfur atom makes a negligible contribution to the Cu extended X-ray absorption fine structure (EXAFS) even in single crystals of plastocyanin oriented so as to maximize its contribution.[4] These results have heightened the interest in Cu-thioether complexes as attempts to understand the electronic and reactivity properties of the blue copper site continue.

Recently, Peerce, Gray, and Anson reported on the coordination chemistry of the ligand thiobis(ethylenenitrilo)tetraacetic acid (TEDTA) with Cr(III).[5] They prepared two different isomers in aqueous solution and proposed mononuclear structures for them on the basis of their spectroscopic properties and reactivity. Here, we report the first structurally characterized complex of this ligand,

(1) Colman, P. M.; Freeman, H. C.; Guss, J. M.; Murata, M.; Norris, V. A.; Ramshaw, J. A. M.; Venkatappa, M. P. *Nature (London)* **1978**, *272*, 319-324.
(2) Adman, E. T.; Stenkamp, R. E.; Sieker, L. C.; Jensen, L. H. *J. Mol. Biol.* **1978**, *123*, 35-47. Adman, E. T.; Jensen, L. H. *Isr. J. Chem.* **1981**, *21*, 8-12.
(3) Freeman, H. C. *Coord. Chem.* **1981**, *21*, 29-51.
(4) Scott, R. A.; Hahn, J. E.; Doniach, S.; Freeman, H. C.; Hodgson, K. O. *J. Am. Chem. Soc.* **1982**, *104*, 5364-5369.
(5) Peerce, P. J.; Gray, H. B.; Anson, F. C. *Inorg. Chem.* **1979**, *18*, 2593-2599.

0020-1669/86/1325-1800$01.50/0